

# Direct growth of densely aligned ZnO nanorods on graphene

Mitsuhiro Honda, Ryuji Okumura, and Yo Ichikawa

Graduate School of Engineering, Nagoya Institute of Technology, Nagoya 466-8555,  
Japan

Densely aligned ZnO nanorods were directly grown on graphene sheets. On graphene prepared via a chemical vapor deposition technique, ZnO nanorods were synthesized by a hydrothermal method. The rod density was  $\sim 1.4 \times 10^9 / \text{cm}^2$  and the nanorods were observed to be well aligned on graphene by scanning electron microscopy. The formation of such ZnO structures is considered to be induced by carbon vacancies in graphene in accordance with Raman spectroscopic results.

Zinc oxide (ZnO) is one of the most attractive semiconductors for combining with graphene owing to its application to physical and chemical sensors, ultraviolet (UV) lasers and photodetectors, light-emitting diodes, and many other optoelectronic devices.<sup>1-4)</sup> ZnO nanostructures such as nanowires, nanowalls, nanotubes and nanorods have been grown on graphene through gas and liquid phase processes.<sup>5-7)</sup> In comparison with gas phase methods such as chemical vapor deposition (CVD), the liquid-phase synthesis is known as a route with less damage to the platforms of graphene and technologically important substrates such as plastics and glasses due to the less reactivity of the solution and the low reaction temperature (~80 °C). Liquid-phase methods generally require the formation of ZnO seed layers at the graphene surface to initiate the nucleation of ZnO.<sup>8)</sup> The seed layer becomes a ZnO-graphene hybrid junction, which is likely to induce less efficient carrier transportation between them.<sup>9)</sup> Furthermore, the seeding process, the exposure of graphene in chemicals at elevated temperatures, may generate unintended defects, which spoil its high electrical conductivity and optical transmittance. Recent studies show the growth of ZnO nanorods on graphene without seeding layers via liquid-phase methods.<sup>3, 10, 11)</sup> Currently, there is room for the improvement of rod orientation and the additional optimization of density and size for the practical use of ZnO-graphene hybrids in devices.

Here, we report the direct growth of highly dense ZnO nanorods with orientation on graphene substructures. Graphene was synthesized by atmospheric pressure CVD (APCVD).<sup>12)</sup> On the prepared graphene basis, a hydrothermal synthesis was conducted to produce ZnO nanorods.

The density of nanorods increased to  $1.4 \times 10^9/\text{cm}^2$  and the rod orientation was improved. The density and orientation of produced nanorods were considered to be attributed to the defects of the graphene surface in accordance with the Raman spectroscopy results of graphene.

Figure 1(a) shows a schematic illustration of an experimental setup for APCVD for graphene preparation using solid camphor as a carbon source. Camphor (3 mg) and a Cu foil (99.9%, 0.010 mm thick) are placed in a quartz tube separately for individual heating using Furnaces 1 and 2. Firstly, a gas mixture consisting of hydrogen and argon (20:80) at 100 sccm started flowing in the tube. The temperature at Furnace 2 elevated to 1000 °C at a rate of 30 °C per minute. After the temperature reached 1000 °C, the Cu foil was continuously heated for 30 min to reduce the Cu defect concentration, obtain a flatter Cu surface, and increase the crystal domain size. Then, camphor was evaporated by heating at 200 °C and was introduced to high-temperature zone by flowing the Ar-H<sub>2</sub> (98:2) gas mixture at 200 sccm. Here, the Cu foil temperatures of 800 and 1000 °C were examined. Graphene growth was completed in 10 min and furnaces were naturally cooled to room temperature.

Figure 1(b) indicates the schematic diagram of the following procedure to form graphene on a quartz substrate and grow ZnO nanorods on it. The graphene film prepared on the Cu foil was transferred onto a substrate by a wet transfer technique.<sup>13)</sup> Then, on the graphene film, ZnO nanorods were synthesized following a hydrothermal method.<sup>14)</sup> A graphene-transferred substrate was immersed in the mixture of zinc nitrite hexahydrate (0.1 M, 50 mL) and sodium hydroxide (1.5 M, 50 mL) solutions. By heating the solution at 90 °C for 2 h, a hydrothermal

reaction was induced. The prepared graphene and ZnO nanorods were characterized by UV-vis spectrometry (Shimazu UVmini-1240), Raman spectroscopy (JASCO NRS-3300) and scanning electron microscopy (SEM; JEOL JSM5600).

Figure 2(a) shows transmittance spectra of graphene samples using two different Cu substrate temperatures, namely, 800 and 1000 °C. In both spectra, the characteristic peak assigned to C=C bonds in aromatic rings is observed at 266 nm, which is typically seen in graphene samples.<sup>15)</sup> Based on transmittance at 633 nm, the number of layers is estimated to be 4 and 12 for the samples prepared with 800 and 1000 °C, respectively.<sup>16)</sup> Later in this paper, 4- and 12-layer graphene samples are named as few- and multi-layer graphenes (FLG and MLG). Our MLG sample, which exhibits more than 10 layers, is expected to function as a transparent conductive layer.

Through transmittance measurements of graphene, the number of layers was found to be affected by Cu substrate temperature. A high substrate temperature was observed to produce graphene with multiple layers. In the high-temperature zone, by applying heat to camphor molecules at a substrate, carbon-related species are generated by pyrolytic decomposition.<sup>17)</sup> The rate of decomposition is expected to increase with a higher thermal energy given to camphor molecules, leading to a much higher amount of carbon source for graphene synthesis. Hence, MLG was synthesized from many resources at high temperature substrates.

Figure 2(b) represents Raman spectra of prepared graphenes. Red and blue curves correspond to FLG and MLG, respectively. Graphene peaks are located at 1350, 1600, and 2700  $\text{cm}^{-1}$ , which

are referred to as D, G, and 2D bands, respectively.<sup>18)</sup> We note that, in the spectrum of MLG, the D' band is seen to locate at  $1628\text{ cm}^{-1}$ , overlapping with the G band.<sup>19)</sup> The D and D' bands are formed by disorders, while the G and 2D bands are indicative of  $sp^2$  in graphene.

The intensity ratio of the D band to the G band (D/G) in FLG is calculated to be 0.17 through curve fitting with a Lorentz function. On the other hand, MLG shows a D/G value equal to 0.96. It was found that defect-free graphene was prepared at  $800\text{ }^\circ\text{C}$ , while a highly defective product was obtained at  $1000\text{ }^\circ\text{C}$ . In addition, since the intensity ratio of the D' band to the G band is 0.31, Raman features of defects in MLG are expected to be caused by carbon vacancy.<sup>19)</sup>

The defect formation in graphene is considered to be associated with the pyrolysis of camphor molecules or graphene during synthesis. At  $800\text{ }^\circ\text{C}$ , methyl groups in camphor dissociate easily with remaining structures of hexagonal and pentagonal rings. At around  $1000\text{ }^\circ\text{C}$ , it is expected that camphor molecules will be pyrolyzed and cracked carbon species will be produced<sup>20)</sup>, or the formed graphene will be thermally decomposed during synthesis on a Cu foil. Thus, highly defective graphene was produced on a high-temperature substrate.

Figure 3(a) shows a photograph of graphene samples after ZnO synthesis. The sizes of the substrate and graphene used are  $15 \times 10\text{ mm}^2$ , and  $10 \times 7\text{ mm}^2$ , respectively. In Fig. 3(a), the gray area indicates the transferred graphene (MLG) on a quartz substrate. Graphene is seen to remain on the substrate after hydrothermal synthesis. Figs. 3(b) and 3(c), and 3(d) are SEM images of ZnO nanorods on MLG and FLG, respectively. ZnO nanorods are observed to distribute densely and uniformly on MLG, while the nanorods on FLG are seen to be sparse.

The density of nanorods on MLG is measured to be  $(1.4 \pm 0.2) \times 10^9 / \text{cm}^2$ , which is comparable to those obtained by seed growth methods.<sup>21)</sup> The rod diameter is  $(190 \pm 10)$  nm. On FLG, ZnO nanorods are grown radially from the specific points as seen in Fig. 3(d). The rod density on FLG is observed to be quite less than that on MLG. Taking into account the distinction in the defect fraction between FLG and MLG, in our experiments, carbon vacancy defects are considered to serve as seeds for ZnO nanorod growth instead of the seeding layers used in conventional methods. According to the results of the previous studies on ZnO nanostructure growth and graphene defects, the synthetic reaction is proposed to be initiated at the defects of graphene.<sup>3, 22, 23)</sup> Because the reactivity at the defects on graphene is locally increased, hydroxyl groups (OH<sup>-</sup>) contained in the solution used during hydrothermal growth attach easily to those defect sites, leading to nucleation and ZnO growth on them. Therefore, the nanorod density is expected to be higher with an increase in the defect fraction.

Finally, the prepared product was observed by Raman spectroscopy. In Fig. 4, curve (i) represents the Raman spectrum of ZnO nanorods grown on graphene. For comparison, the Raman spectrum of ZnO nanorods prepared via a seed growth method was also measured, which is shown as curve (ii) in Fig. 4. As indicated by filled stars in Fig. 4, typical peaks of graphene, D-, G-, and 2D bands, are seen in spectrum (i). This indicates that nanorods are grown on graphene without any crucial changes to its structure. An intense and sharp peak at  $440 \text{ cm}^{-1}$  denotes the wurtzite lattice of ZnO nanorods. Side peaks at  $339$  and  $594 \text{ cm}^{-1}$  are also typical Raman features of ZnO, corresponding to second-order scattering and the  $A_1$  (LO) mode,

respectively.<sup>24)</sup> Those peaks derived from ZnO are observed in both spectra and the difference between them seems to be negligible. Thus, the data shown in Fig. 4 indicate that ZnO nanorods equivalent to those prepared on a seed layer appear to be produced with graphene being unchanged after the growth.

In conclusion, we demonstrated the direct growth of densely aligned ZnO nanorods on graphene via a hydrothermal approach. Through SEM observation, the density and diameter of produced nanorods were found to be  $1.4 \times 10^9 /\text{cm}^2$  and 190 nm, respectively. Densely distributed nanorods were grown on defective graphene, but hardly on defect-free graphene. By Raman spectroscopy, the crystalline state of produced nanorods was confirmed to be equivalent to that grown on the seeding layer. Graphene-ZnO nanorod structures prepared in our experiments are expected to be promising for photonic and optoelectronic devices.

#### Acknowledgements

This work was financially supported by a JSPS Grant-in-Aid for Scientific Research (C) No. 26390102. We thank G. Kalita and M. Tanemura for helpful discussions.

## Reference list

- <sup>1)</sup> C. J. Lee, T. J. Lee, S. C. Lyu, Y. Zhang, H. Ruh, and H. J. Lee, *Appl. Phys. Lett.*, **81**, 3648 (2002).
- <sup>2)</sup> S. W. Hwang, D. H. Shin, C. O. Kim, S. H. Hong, M. C. Kim, J. Kim, K. Y. Lim, S. Kim, S. H. Choi, K. J. Ahn, G. Kim, S. H. Sim, and B. H. Hong, *Phys. Rev. Lett.*, **105**, 127403 (2010).
- <sup>3)</sup> J. Liu, R. Liu, G. Xu, J. Wu, P. Thapa, and D. Moore, *Adv. Funct. Mater.*, **23**, 4941 (2013).
- <sup>4)</sup> K. Chung, C. H. Lee, and G. C. Yi, *Science*, **330**, 655 (2010).
- <sup>5)</sup> Z. Yin, S. Wu, X. Zhou, X. Huang, Q. Zhang, F. Boey, and H. Zhang, *Small*, **6**, 307 (2009).
- <sup>6)</sup> S. Wu, Z. Yin, Q. He, X. Huang, X. Zhou, and H. Zhang, *J. Phys. Chem. C*, **114**, 11816 (2010).
- <sup>7)</sup> B. Kumar, K. Y. Lee, H-K. Park, S. J. Chae, Y. H. Lee, and S-W. Kim, *ACS Nano*, **5**, 4197 (2011).
- <sup>8)</sup> H. X. Chang, Z. H. Sun, K. Y. F. Ho, X. M. Tao, F. Yan, W. M. Kwok, and Z. J. Zheng, *Nanoscale*, **3**, 258 (2011).
- <sup>9)</sup> C. Xu, J-H. Lee, J-C. Lee, B-S. Kim, S. W. Kim, S. W. Hwang, and D. Whang, *CrystEngComm*, **13**, 6036 (2011).
- <sup>10)</sup> N. S. A. Aziz, M. R. Mahmood, K. Yasui, and A. M. Hashim, *Nanoscale Res. Lett.*, **9**, 95 (2014).
- <sup>11)</sup> S. B. Ambade, R. B. Ambade, W. Lee, R. S. Mane, S. C. Yoon, and S-H. Lee, *Nanoscale*, **6**, 12130 (2014).

- <sup>12)</sup> S. Sharma, G. Kalita, M. E. Ayhan, K. Wakita, M. Umeno, and M. Tanemura, *J. Mater. Sci.*, **48**, 7036 (2013).
- <sup>13)</sup> X. Li, Y. Zhu, W. Cai, M. Borysiak, B. Han, D. Chen, R. D. Piner, L. Colombo, and R. S. Ruoff, *Nano Lett.*, **9**, 4359 (2009).
- <sup>14)</sup> Y.-J. Kim, Hadoyawarman, A. Yoon, M. Kim, G.-C. Yi, and C. Liu, *Nanotechnology*, **22**, 245603 (2011).
- <sup>15)</sup> Y. Gui, J. Yuan, W. Wang, J. Zhao, J. Tian, and B. Xie, *Materials*, **7**, 4587 (2014).
- <sup>16)</sup> L. Wu, S. Chu, W. S. Koh, and E. P. Li, *Opt. Express*, **18**, 14395 (2010).
- <sup>17)</sup> P. R. Somani, S. P. Somani, and M. Umeno, *Chem. Phys. Lett.*, **430**, 56 (2006).
- <sup>18)</sup> L. M. Malard, M. A. Pimenta, G. Dresselhaus, and M. S. Dresselhaus, *Phys. Rep.*, **473**, 51 (2009).
- <sup>19)</sup> A. Eckmann, A. Felten, A. Mishchenko, L. Britnell, R. Krupke, K. S. Novoselov, and C. Casiraghi, *Nano Lett.*, **12**, 3925 (2012).
- <sup>20)</sup> M. Sharon, S. Jain, P. D. Kichambare, and M. Kumar, *Mater. Chem. Phys.*, **56**, 284 (1998).
- <sup>21)</sup> W. I. Park, D. H. Kim, S. W. Jung, and G.-C. Yi, *Appl. Phys. Lett.*, **80**, 4232 (2002).
- <sup>22)</sup> F. Banhart, J. Kotakoski, and A. Krasheninnikov, *ACS Nano*, **5**, 26 (2011).
- <sup>23)</sup> R. Viswanatha, P.K. Santra, C. Dasgupta, and D. D. Sarma, *Phys. Rev. Lett.*, **98**, 255501 (2007).
- <sup>24)</sup> G. M. Kumar, P. Ilanchezhian, J. Kawakita, M. Subramanianm, and R. Jayavel, *CrystEngComm*, **12**, 1887 (2010)

## Figure captions

Fig. 1. (Color online) (a) Schematic illustration of an experimental setup for atmospheric pressure chemical vapor deposition to prepare graphene samples. (b) Schematic diagram depicting the formation of graphene on a quartz substrate and growth of ZnO nanorods via hydrothermal method.

Fig. 2. (Color online) (a) Transmittance and (b) Raman spectra of FLG (red) and MLG (blue). In panel (b), D, G, and 2D bands of graphene are shaded by green, orange, and pink, respectively.

Fig. 3. (Color online) (a) Photograph of a ZnO nanorods sample prepared on a quartz substrate on which MLG was transferred. The substrate size is 15 cm x 10 cm<sup>2</sup>. The dark gray rectangle indicates the area covered by graphene. (b, c) SEM images of ZnO nanorods grown on MLG. (d) SEM image of ZnO nanorods grown on FLG.

Fig. 4. (Color online) Raman spectra of ZnO nanorods on MLG and a R-plane sapphire

substrate as a reference, which are marked by (i) and (ii), respectively. Filled and unfilled stars

indicated in the figure denote peaks of graphene and ZnO nanorods, respectively.

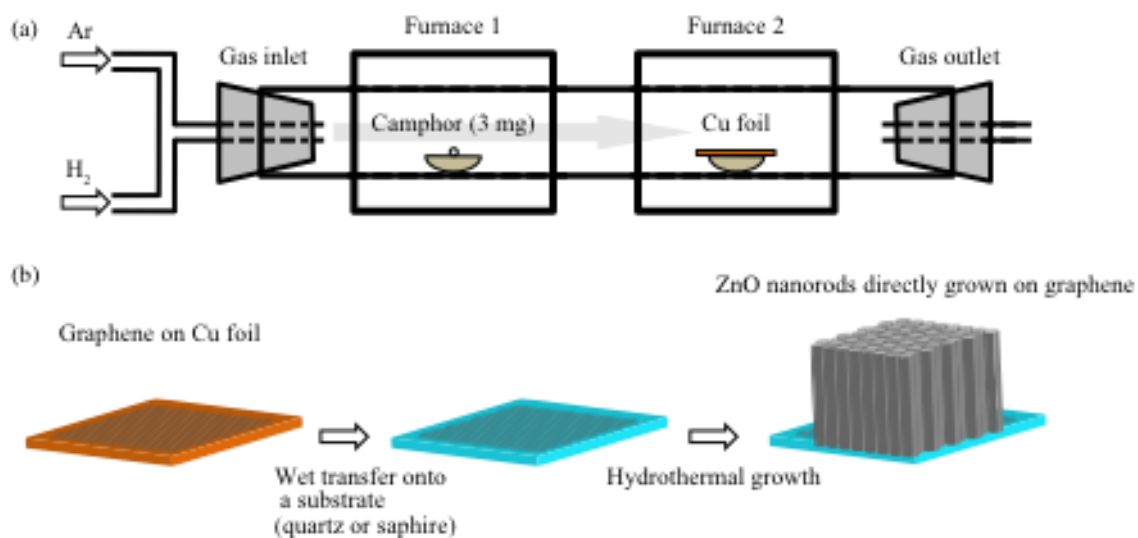


Figure 1

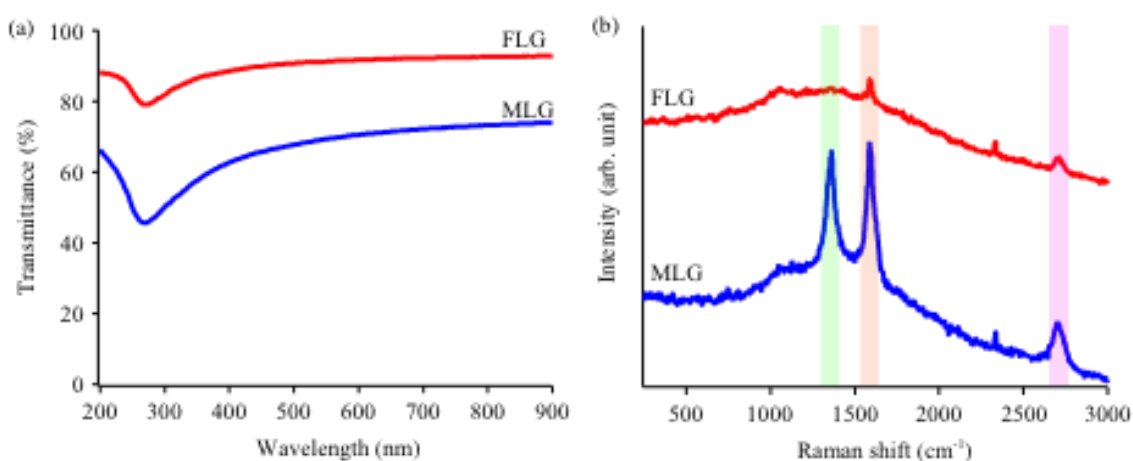


Figure 2

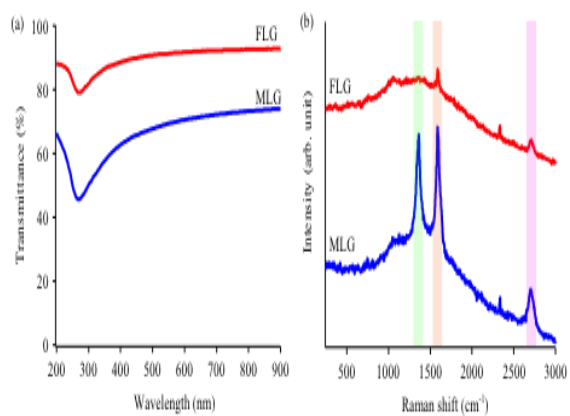


Figure 3

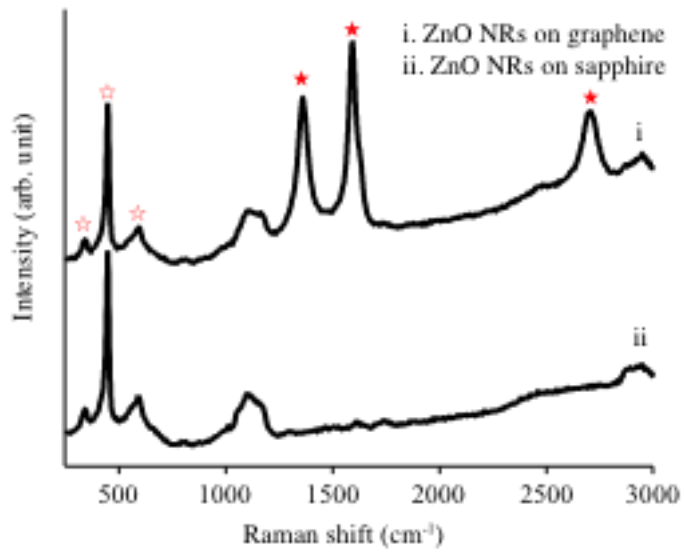


Figure 4